J|A|C|S
ARTICLES
Published on Web 11/28/2002

# Mesomorphism, Isomerization, and Dynamics in a New Series of Pyramidic Liquid Crystals

Herbert Zimmermann,[†] Victoria Bader,[†] Raphy Poupko,[‡] Ellen J. Wachtel,[‡] and Zeev Luz*[,‡]

*Contribution from the Max-Planck-Institut für Medizinische Forschung, Jahnstrasse 29, 69120 Heidelberg, Germany, and Weizmann Institute of Science, Rehovot, 76100, Israel*

Received June 27, 2002

***Abstract:*** Nona-alkanoyloxy tribenzocyclononene (CTV-*n*, where *n* is the number of carbons in the side chains) were prepared for $n = 2$ to 14. The homologues of this series appear in two stable isomeric forms, rigid crown and flexible saddle. We report on their isomerization equilibria and dynamics in solution and on their mesomorphic properties in the neat state. The crown-saddle equilibrium and interconversion kinetics of the CTV-8 isomers were studied in dimethyl formamide solutions using high-resolution $^1$H NMR in the temperature range from 50 to 130 °C. At lower temperatures, the isomerization is too slow to measure. In this range the equilibrium saddle fraction increases from ~0.40 to ~0.65, whereas the isomerization rate increases from $\sim 10^{-4}$ to ~1 $s^{-1}$. The saddle isomer undergoes fast pseudorotation at room temperature, but below about −50 °C, it becomes slow enough to affect the NMR line width. The rate parameters for this process were estimated from the carbon-13 spectra in methylene chloride solutions to be, $k_p$(−100 °C) $\approx 1.7 \times 10^3$ $s^{-1}$ and $E_a \approx 9.6$ kJ/mol. The slow crown-saddle isomerization at room temperature (half-life of about one year) allows quantitative separation (by chromatography) of the two isomers and their separate investigation. When the alkanoyloxy side chains are sufficiently long both isomers are mesogenic ($n \geq 4$ for the saddle and $n \geq 5$ for the crown), exhibiting hexagonal columnar mesophases. The structure, dynamics, and mesomorphic properties of these mesophase were investigated by X-ray diffraction, optical polarizing microscopy, differential scanning calorimetry, and NMR. The lattice parameters of the crown and saddle mesophases of corresponding homologues are almost identical and increase monotonically with increasing length of the side chains. The clearing temperatures of the saddle isomers are consistently lower than those of the corresponding crowns. Within each series, the clearing temperatures are almost independent of the length of the side chains (156 to 170 °C for the crown and 115 to 148 °C for the saddle). The thermal and kinetic properties of the neat compounds lead to peculiar phase sequences, as observed in the polarizing microscope and in the DSC thermogram, involving repeated, back and forth, interconversion between the two isomers. Carbon-13 MAS NMR measurements of the crown and saddle mesophases of several homologues were carried out. The spectra of the crown mesophase exhibit dynamic features consistent with planar 3-fold molecular jumps about the column axes. A quantitative analysis for the CTV-8 crown homologue yielded the following Arrhenius parameters, $A = 3.1 \times 10^{22} s^{-1}$ and $E_a = 130.1$kJ/mol. These unusually high values suggest that the barrier to the jump process is temperature dependent, decreasing with increasing temperature. The rate of this 3-fold jump process is slower for the lower homologues and faster for the higher ones. In contrast, the saddle isomers in the mesophase do not show dynamic effects in their carbon-13 MAS spectra. They do not undergo pseudorotation, and it appears that the molecules remain locked within the columns in a saddle conformation, up to the clearing temperature. However, on (super-)cooling to room temperature and below, selective line broadening is observed in their carbon-13 MAS spectra. This suggests that the saddle conformation is twisted in the mesophase and undergoes fast high-amplitude jumps between the twisted forms. On cooling, these high-amplitude librations freeze out to give an orientationally disordered state. On a very long time scale (of the order of days at 100 °C), the saddle mesophase transforms into that of the crown, apparently by sublimation.

## 1. Introduction

The name pyramidic liquid crystal was originally given to a class of discotic mesogens whose molecules are derived from the hydrocarbon core tribenzocyclononene (see Figure 1a). The parent compound of this series obtained by trimerization of veratryl alcohol, hexa methoxy tribenzocyclononene, is also called cyclotriveratrylene. In the following we shall refer to the structural formula of this core as CTV. When unsubstituted or substituted with six ($R' = H$, $R \neq H$) substituents the core acquires a cone shape, or pyramidic structure. When the substituents, R, consist of sufficiently long side chains linked

[†] Max-Planck-Institut für Mediziniche Forschung.
[‡] Weizmann Institute of Science.


10.1021/ja020889e CCC: $22.00 

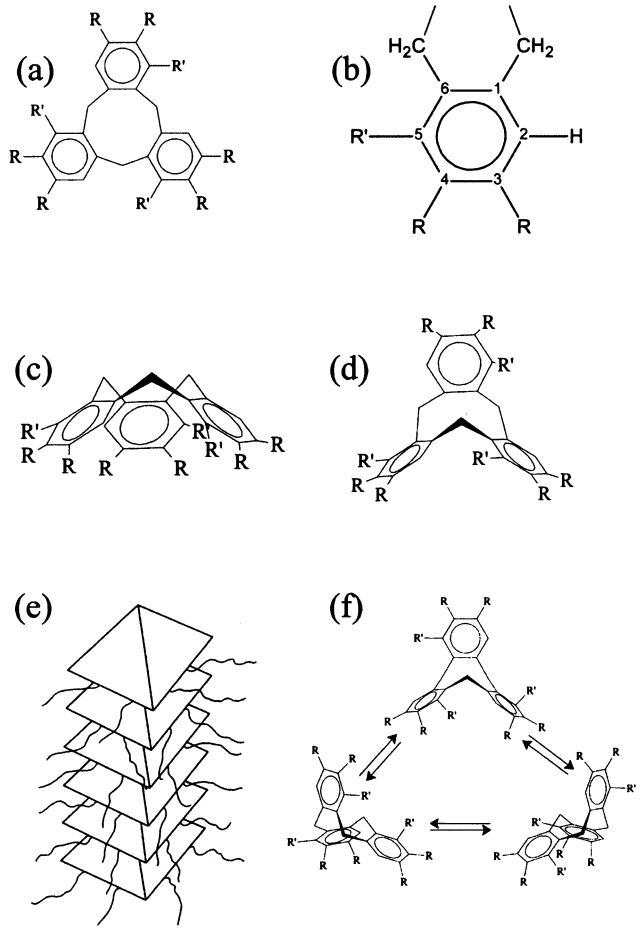


***Figure 1.*** (a) Structural formula of the CTV core, (b) numerical convention used for the aromatic carbons, (c) the structure of the crown conformer, (d) the structure of the saddle conformer, and (e) a schematic view of a column made of pyramidic molecules. (d) Pseudorotation of the saddle isomer.

via ether or ester bonds mesogenic compounds are obtained, which exhibit columnar mesophases of various two-dimensional symmetries (such as hexagonal or rectangular).[1−4] Within the columns, the molecules are stacked on top of each other in a regular arrangement (Figure 1 e), resulting in a macroscopic electric dipole. The optical,[2] electric,[5] ordering,[6] and dynamic[7] properties of these mesophases have been studied extensively by polarizing optical microscopy, electric polarization and NMR methods, providing much insight into the physical properties of these mesophases.

In the present work, we extend the study of this family of liquid crystals to nonasubstituted CTV, with R=R′=OC(O)-$C_{n-1}H_{2n-1}$. We refer to the homologues of this series as CTV-*n*, where n is the number of carbons in the side chains.The increase in the number of substituents from six (R′ = H, R ≠ H, $C_{3v}$ symmetry) to nine (R = R′ ≠ H, $C_3$ symmetry) has two important consequences. One concerns chirality. The molecules now lack symmetry planes and although they do not possess asymmetric tetrahedral carbons they are structurally chiral. Consequently, the as-synthesized compounds consist of racemic mixtures of optical isomers. We were, so far, unable to separate these nonasubstituted derivatives into their enantiomers, although their NMR spectra could be discriminated in chiral nematic solvents.[8] Similar chiral discrimination was observed by circular dichroism in other optically active substituted CTV derivatives.[9]

The second point concerns the conformation of the CTV core. When unsubstituted, or 6-fold substituted (R′ = R = H, or R′ = H, R ≠ H) the crown form (Figure 1c) is apparently the only stable conformation of the CTV moiety. Upon substituting bulky groups in benzene sites *ortho* to the ring methylene (R′ ≠ H) the crown form is destabilized due to steric hindrance with neighboring rings.[10] This leads to the formation of the saddle form (Figure 1d) which has an open structure and is highly flexible. This increases its entropy and correspondingly lowers its free energy. In fact, in solution, at high temperatures, an equilibrium between the crown and saddle forms is established, which greatly favors the saddle isomer. At room temperature and below the equilibrium would favors the crown form, but the isomerization is extremely slow so that the two isomers can readily be separated by column chromatography and their properties studied individually. It turns out that both conformers, with sufficiently long side chains ($n \geq 4$ for the saddle and $n \geq 5$ for the crown) are mesogenic and form similar mesophases. However, their dynamic properties, as reflected in their MAS $^{13}C$ NMR spectra, are quite different. In the following sections, we describe the preparation and separation of these mesogens, their mesomorphic properties as studied by X-ray, differential scanning calorimetry (DSC) and polarizing optical microscopy, as well as their dynamic properties as manifested in their NMR spectra. For completion, we also report on the crown-saddle equilibrium and isomerization kinetics in isotropic solutions.

## 2. Experimental Section

**2.1. Synthesis.** The 1,2,3,6,7,8,11,12,13 CTV-*n* were prepared by esterification of nonahydroxy CTV (CTV−OH) with the corresponding acid chloride (or acid anhydride). Two methods of esterification were employed, at low (0 °C) and high (200 °C) temperatures, respectively. The first method yielded pure crown forms, while the latter resulted in mixtures of saddle and crown, which were separated by column chromatography.

In a typical low-temperature experiment, 200 mg CTV−OH were dissolved in 20 mL dry pyridine and cooled to 0 °C. Two to four mL of acid chloride were added dropwise while stirring for 2 d. The pyridine was then evaporated on a rotavapor (at 40 °C) under reduced pressure (oil pump). The quasi-solid residue was treated with 1N HCl at room temperature, stirred for 1 h and filtered. The filtrate was recrystallized from ethanol, boiled for just a few minutes, followed by chromatographic purification (silica, ether/$CH_2Cl_2$, 1/9). High resolution $^1H$ NMR confirmed the purity of the compound which was entirely in the crown form (an AB quartet at ∼4 ppm for the ring methylene protons). This procedure worked well for the higher homologues from $n \geq 5$, but failed for the lower homologues ($n = 2$ to 4). For the lower members of the series an alternative method was used for preparing the crown

(1) Zimmermann, H.; Poupko, R.; Luz, Z.; Billard, J. *Z. Naturforsch.* **1985**, *40a*, 149−160.
(2) Zimmermann, H.; Poupko, R.; Luz, Z. Billard, J. *Z. Naturforsch.* **1986**, *41a*, 1137−1140.
(3) Malthete, J.; Collet, A. *Nouv. J. Chim.* **1985**, *9*, 151−153.
(4) Levelut, A.-M.; Malthete, J.; Collet, A. *J. Physique* **1986**, *47*, 351−357.
(5) Jakli, A. J.; Saupe, A.; Scherowsky, G. V.; Chen, Xin Hua *Liquid Crystals* **1997**, *22*, 309−316.
(6) Poupko, R.; Luz, Z.; Spielberg, N.; Zimmermann, H. *J. Am. Chem. Soc.* **1989**, *111*, 6094−6105.
(7) Zamir, S.; Luz, Z.; Poupko, R.; Alexander, S.; Zimmermann, H. *J. Chem. Phys.* **1991**, *94*, 5927−5938.
(8) Lesot, P.; Merlet, D.; Sarfati, M.; Courtieu, J.; Zimmermann, H.; Luz, Z. *J. Am. Chem. Soc.* **2002**, *124*, 10 071−10 082.
(9) Garcia, C.; Andraud, C.; Collet, A. *Supramol. Chem.* **1992**, *1*, 31−45.
(10) Collet, A. *Tetrahedron*, **1987**, *43*, 5725−5759.

form. In this version,[11] (dimethylamino)pyridine (DMAP) was employed as catalyst and instead of the acid chloride, the corresponding acid anhydride was used. As an example, we describe the preparation of the crown CTV-2 homologue. CTV−OH (300 mg), 10 mL acetic acid anhydride, and 40 mg DMAP were heated to 50 °C and stirred for 24 h. The excess anhydride was removed by pumping at $10^{-3}$ Torr at room temperature. (For the $n = 3$, the pumping stage was not necessary because, after cooling the reaction mixture a crystalline product was already obtained.) The residue was recrystallized from $CHCl_3/C_2H_5$-OH, followed by column chromatography (silica, $CH_2Cl_2$/ether 1/1) and a second recrystallization, resulting in pure crown CTV-2.

The high-temperature esterification was affected by refluxing (at 200° C) a mixture containing CTV−OH (200 mg) and an excess of the corresponding acid chloride. The refluxing was continued for 50 h, while continuously stirring the mixture. The excess acid chloride was then removed by evaporation under reduced pressure and the residue recrystallized three times from boiling ethanol using charcoal. Thin-layer chromatography (Silica, ether/$CH_2Cl_2$, 1/9) always showed two spots corresponding to the crown and saddle forms. They were quantitatively separated by column chromatography (same composition as for the TLC). High-resolution NMR confirmed the purity of each separated isomer (AB quartet for the crown and a singlet for the saddle at ~4 ppm). This method worked well for all homologues with $n \geq 3$. For the $n = 2$ homologue the procedure was slightly modified: 250 mg of CTV−OH were refluxed for 2 h at 140 °C with 30 mL acetic anhydride to which a drop of concentrated sulfuric acid was added. The excess anhydride was removed as above and the residue was recrystallized from ethanol. The product was predominantly saddle, but contained 15−20% crown. Using column chromatography (silica/ether 1/1) the pure saddle form was finally recovered.

The CTV−OH was obtained by bromination and hydrolysis of nonamethoxy tribenzocyclononene (CTV−$OCH_3$) as follows: To 4 g CTV−$OCH_3$ dissolved in 1.4 L benzene, was slowly (2 h) added 50 mL of $BBr_3$. The solution was protected from humidity and refluxed for 10 d while stirring. During this period, the white precipitate gradually changed to black. After cooling, the excess $BBr_3$ was decomposed by adding 200 to 300 mL of water over a period of 5 h. The mixture was then stirred overnight and finally passed through a glass filter. The filtrate was treated with 250 mL water and boiled for 1 h. Acetone was then added to dissolve the solid formed. The clear solution was then boiled until all the acetone evaporated and crystals of CTV−OH started to precipitate. The boiling was continued for a while, followed by cooling, filtering, and drying of the crystals (long needles) on a vacuum manifold. Yield, 2.9 g. $^1$H NMR in DMSO-$d_6$ showed the expected spectrum of the crown form with three distinct OH peaks.

CTV−$OCH_3$ was obtained from 3,4,5-trimethoxy benzyl alcohol by condensation.[12] Thirty grams of the latter compound were dissolved in 600 mL 10% aqueous $H_2SO_4$ and refluxed under stirring for 6 h. The precipitated solid was separated by decantation and triturated with about 300 mL ether until a crystalline powder was obtained. The filtered product was then crystallized several times from ethanol. Yield, 3.4 g, mp 201−203 °C, *m.z.* 540. $^1$H NMR indicated high purity clock-wise substituted crown form ($C_3$ symmetry).

We complete this section by referring to the review article of Collet,[13] where the synthesis of many other substituted CTV compounds is described.

**2.2. Physical Characterization and NMR Measurements.** Differential scanning calorimetry (Mettler DSC30), optical polarizing microscopy (Zeiss Universal with a Mettler FP52 heating stage) and X-ray diffraction (Cu-radiation, $\lambda$=1.54 Å, using Fuji imaging plates) measurements were performed as described in detail earlier.[14] For the latter experiments, the specimens were placed in a horizontal (0.7 T) magnetic field, perpendicular to the X-ray beam direction. High-resolution $^1$H and $^{13}$C NMR spectra were recorded on a DRX-400 Bruker spectrometer operating at 400.13 and 100.62 MHz, respectively. The $^{13}$C magic angle spinning (MAS) NMR measurements were performed on a solid-state DSX-300 Bruker spectrometer equipped with 4 or 7 mm probes and a BVT-3000 temperature controller. Spectra were recorded using either cross polarization (CP; contact time, 2 ms) or single pulse excitation ($\pi$/2 pulse width 4 or 6 $\mu$s). The temperature was calibrated using $Pb(NO_3)_2$.[15]

## 3. Mesomorphic and Thermodynamic Properties

**3.1. Crown-Saddle Isomerization in Solution.** Before discussing the mesomorphic properties of the neat CTV-n mesogens, we briefly describe their thermodynamic characteristics in isotropic solutions. As indicated in the Experimental Section, the conformation of the as-synthesized product depended on whether the synthesis was performed by the low or high temperature method. The low-temperature method yielded a product that was entirely in the crown form, thus preserving the conformation of the starting materials, CTV−OH and CTV−$OCH_3$. On the other hand, the high temperature esterification always yielded a mixture of the crown and saddle isomers, with the latter dominating. These results indicate that the crown-saddle isomerization is slow on the time scale of the low-temperature synthesis and purification procedure (several hours/days, including relatively short periods of dissolving the material at 40 °C and recrystallization from boiling ethanol), while it is fast under the conditions of the high-temperature synthesis (200 °C). The slow interconversion at room temperature made it possible to quantitatively separate the two isomers by room-temperature column chromatography and purify them separately without fear of isomerization. In this section, we study the crown-saddle isomerization kinetics and equilibria in isotropic solutions at high temperatures, using real-time $^1$H NMR intensity measurements. Such measurements are feasible for reaction half-lives of the order minutes to several hours (or even days).

On the left-hand side of Figure 2 are shown room-temperature high-resolution $^1$H NMR spectra (low-field parts only) of the pure crown, pure saddle and a mixture of both isomers for the CTV-8 homologue dissolved in chloroform-*d*. The side chain aliphatic hydrogens (not shown) exhibit a multitude of signals in the range 0.5 to 3 ppm. The peaks at around 4 ppm are due to the ring methylene protons. In the crown isomer their spectrum is an AB quartet as expected for a rigid structure with $C_3$ symmetry, with $\delta^{in} = 4.44$ ppm and $\delta^{out} = 3.76$ ppm and $^3J_{H^{in}H^{out}} = 14.3$ Hz, where *in* and *out* indicate the inner and outer methylene hydrogens. Their identification as $\delta^{in}$ and $\delta^{out}$ is based on deuterium spectra in liquid crystalline solutions.[8] In the saddle conformer these protons exhibit a sharp singlet (at 3.9 ppm), reflecting the fast pseudorotation (see Figure 1f) of this conformer, which leads to an average $C_{3h}$ symmetry. The aromatic hydrogens of the unsubstituted sites in the benzene rings appear at 7.6 ppm for the crown form and at 6.9 ppm for the saddle conformer. We have used the latter peaks to monitor the crown-saddle equilibrium and interconversion kinetics in solution. Quantitative measurements were performed only on the CTV-8 homologue. The experiments were done at high

(11) Höfle, G.; Steglich, W.; Vorbrüggen, H. *Angew. Chem., Int. Ed. Engl.* **1978**, *17*, 569−583.
(12) Bosch, J.; Canals, J.; Granados, R. *Anals de Quimica*, **1976**, *22*, 709−712.
(13) Collet, A. In *Comprehensive Supramolecular Chemistry*; Atwood, J. L., Davies, J. E. D., Macnicol, D. D., Vögtle, F., Eds.; Vol. 6, 1996; 281−303.
(14) Callucci, L.; Zimmermann, H.; Wachtel, E. J.; Poupko, R.; Luz, Z. *Liquid Crystals* **1997**, *22*, 621−630.
(15) Bielecki, A.; Burum, D. P. *J. Magn. Res.* **1995**, *A116*, 215−220.

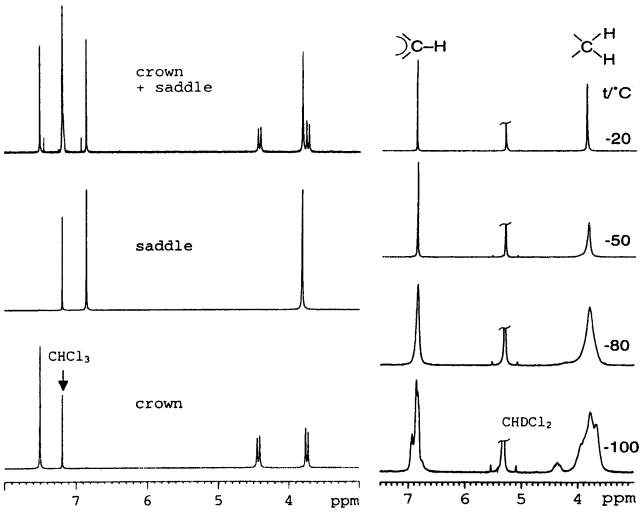


***Figure 2.*** Left: Proton high-resolution NMR spectra of CTV-8 in $CDCl_3$ in the range 3 to 8 ppm. From bottom to top: Crown isomer; saddle isomer; a mixture of both isomers. Right: Proton high-resolution NMR spectra of the saddle isomer of CTV-8 in $CD_2Cl_2$ as a function of the temperature as indicated.

temperatures, starting with a solution of one of the pure isomers and monitoring the changes in the proton NMR spectra as the system approached equilibrium in real time.

For the analysis of the kinetic and thermodynamic properties in solution we define the equilibrium

$$\text{crown} \underset{k_2}{\overset{k_1}{\rightleftharpoons}} \text{saddle} \tag{1}$$

and set up the kinetic equations for each isomer

$$\frac{dC(t)}{dt} = -k_1C(t) + k_2S(t) \tag{2}$$

$$\frac{dS(t)}{dt} = k_1C(t) - k_2S(t)$$

where $C(t)$ and $S(t)$ are, respectively, the fractional concentrations of the crown and saddle isomers at time $t$ of the reaction. Integration of eq 2 yields

$$\frac{C(t) - C(\infty)}{C(0) - C(\infty)} = -\frac{S(t) - S(\infty)}{S(0) - S(\infty)} = e^{-\mathrm{kt}} \tag{3}$$

or more conveniently for practical implementation

$$\frac{[S(\infty) - S(t)] - [C(\infty) - C(t)]}{[S(\infty) - S(0)] - [C(\infty) - C(0)]} = e^{-\mathrm{kt}} \tag{4}$$

where $C(\infty)$ and $S(\infty)$ are the equilibrium fractional concentrations of the crown and saddle isomers

$$k = k_1 + k_2 \text{ and } \frac{S(\infty)}{C(\infty)} = \frac{k_1}{k_2} = K \tag{5}$$

In practice, we started the experiments by inserting a solution of pure crown or pure saddle in the NMR spectrometer which was preheated to the desired temperature. The approach to equilibrium was then followed by recording and monitoring the NMR peak intensities at selected times. Kinetic measurements could be carried out in the temperature range from 50 to 90 °C.

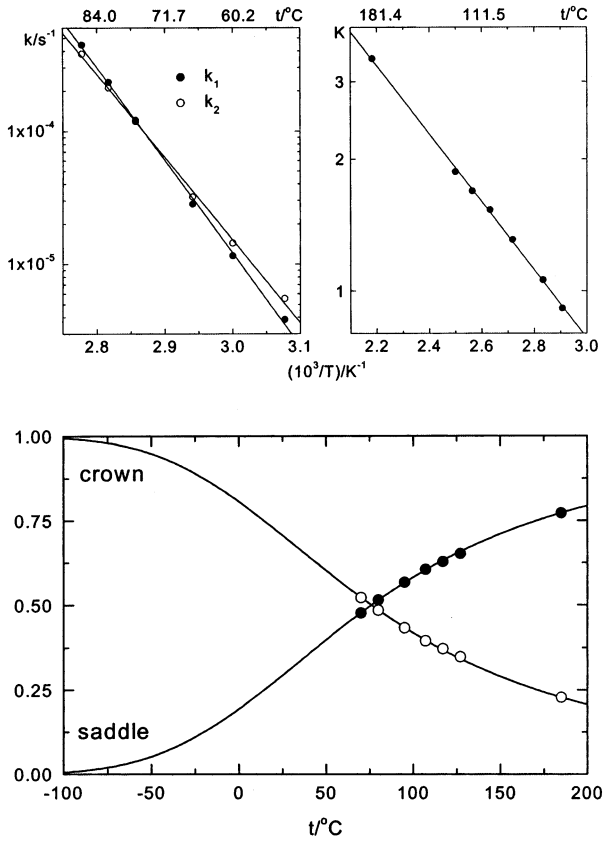


***Figure 3.*** Top: Plots of the isomerization rate constants (left) and equilibria (right) of the crown-saddle system of CTV-8 in DMF-$d_7$ solutions as a function of the inverse absolute temperature. Bottom: Fractional equilibrium populations of the crown and saddle isomers in the CTV-8/DMF-$d_7$ solution as a function of the temperature. The points at 185 °C correspond to a measurement in the melt. Solid and open symbols are experimental, whereas the full lines are calculated from the thermodynamic data given in the text.

Below and above this range, the isomerization was either too slow or too fast to measure by this method. The equilibrium constant measurements could, however, be extended up to 130 °C. Plots of the rate and equilibrium constants versus the inverse absolute temperature are shown in the top part of Figure 3. The K-plot also includes a point at 185 °C, which was obtained by quenching the neat melt down to room temperature. They were analyzed in terms of the Boltzmann absolute rate theory equations

$$K = e^{\Delta S/R}e^{-\Delta H/RT} \qquad k_\mathrm{j} = \frac{k_\mathrm{B}T}{h}e^{\Delta S_\mathrm{j}^{\neq}/R}e^{-\Delta H_\mathrm{j}^{\neq}/RT}$$

yielding the following results (for CTV-8)

$$\Delta H = 15.1 \pm 0.2 \text{ kJ/mol}$$
$$\Delta H_1^{\neq} = 131.8 \pm 2.5 \text{ kJ/mol}$$
$$\Delta H_2^{\neq} = 116.7 \pm 2.5 \text{ kJ/mol}$$

$$\Delta S = 42.7 \pm 0.5 \text{ JK}^{-1}\text{ mol}^{-1}$$
$$\Delta S_1^{\neq} = 55.2 \pm 7.1 \text{ JK}^{-1}\text{ mol}^{-1}$$
$$\Delta S_2^{\neq} = 12.5 \pm 7.2 \text{ JK}^{-1}\text{ mol}^{-1}$$

Also shown in the figure (bottom part) are plots of the equilibrium fractional populations of the crown and saddle isomers as a function of the temperature, calculated from the

***Table 1.*** Melting (mp) and Clearing (c.p.) Temperatures (°C), and in Brackets the Transition Enthalpies (kJmol$^{-1}$) for the Crown (C) and Saddle (S) CTV-*n* Homologues Studied in the Present Work

| | n | 2 | 3 | 4 | 5 | 6 | 7 | 8 | 9 | 10 | 11 | 12 | 13 | 14 |
|---|---|---|---|---|---|---|---|---|---|---|---|---|---|---|
| C | mp | 218 | 193 | 177 | | 25 | 19 | 45 | 39 | 43 | 44 | 60 | 65 | 71 |
| | $\Delta H$ | | (85) | (64) | | (3) | (4) | (24) | (19) | (58) | (62) | (93) | (117) | (137) |
| | c.p. | | | | 164 | 162 | 170 | 164 | 160 | 160 | 164 | 159 | 160 | 156 |
| | $\Delta H$ | | | | (52) | (46) | (56) | (59) | (56) | (56) | (56) | (41) | (54) | (58) |
| S | mp | 248 | 67.5 | | | | | | | | | | | |
| | $\Delta H$ | (61.0) | (5.5) | | | | | | | | | | | |
| | c.p.[a] | | | 148 | 135 | 135 | 127 | 137 | 115 | 125 | 128 | 126 | 126 | 126 |

[a] These temperatures correspond to the minima in the first endothermic transition in the DSC thermogram, (see Figure 5).

above results. Thus, despite the steric hindrance of the *ortho* substituents, the more stable species at lower temperatures is still the crown form, due to its lower enthalpy. On the other hand, the high flexibility of the core and the increased number of side chain conformations associated with the more open structure of the saddle isomer, increases its entropy, rendering it the more stable species at higher temperatures. Extrapolation of the results show that the half-life for the crown-saddle isomerization in solution is of the order of a year at room temperature, about 100 years at 0 °C and more than the age of the universe at −100 °C. Similar kinetic parameters were reported for the racemization of chiral hexasubstituted crown CTV derivatives.[16] As we shall see in the following, the reaction remains slow in the solid and in the mesophase, even at high temperatures, leading to very special effects on the phase diagram of the neat compounds.

Finally, we comment on the low-temperature proton NMR spectra of solutions of the CTV-8 isomers in $CD_2Cl_2$. The results for the saddle isomer are shown on the right-hand side of Figure 2. At around −50 °C, they exhibit line broadening that suggest the slowing down of the pseudorotation process. Between about −80 °C and −100 °C the NMR peaks show structures, which, however, cannot straightforwardly be interpreted in terms of freezing out of the pseudorotation. The situation is complicated by the observation of line splitting also in the low temperature spectra of the crown isomer, which is not expected to show dynamic effects. We therefore tentatively ascribe these structures, at least partly, to distortions of the ideal structures of the saddle and crown forms, perhaps due to complexation with the solvent. We have observed line splittings effects also in the low-temperature carbon-13 spectra of these isomer. We discuss them in Section 5 below.

**3.2. Phase Diagrams: DSC and Polarizing Optical Microscopy.** We have determined the phase diagrams of the neat crown and saddle isomers of the entire series of CTV-*n* homologues from $n = 2$ to 14, using DSC and optical polarizing microscopy. The saddle conformers from $n = 4$ to 14 and the crown conformers from $n = 5$ to 14 are all mesogenic, exhibiting a single columnar hexagonal mesophase. Clearing temperatures, and for the crown isomers (with $n \geq 6$) also melting temperatures, as well as corresponding enthalpies are summarized in Table 1. The transition temperatures are also plotted as a function of the chain length in Figure 4. Invariably the clearing temperatures of the crown isomers are higher than those for the corresponding saddle. In fact the variation in the clearing temperatures within each series (156 to 170 °C for the crown series and 115 to 148 °C for the saddle) is smaller than the

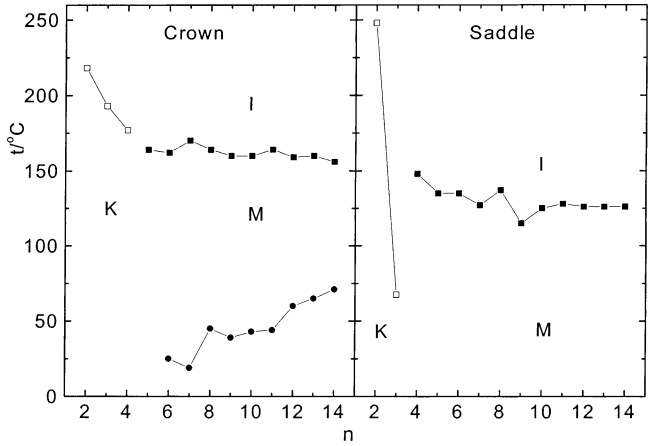


***Figure 4.*** Phase diagrams for the crown (left) and saddle (right) isomers of CTV-*n* for the $n = 2$ to 14 homologues. The letters K, M, and I stand for, crystalline phase; hexagonal columnar mesophase and isotropic melt. Open symbols are melting points of nonmesognic homologues; solid circles are solid to mesophase transitions (observed only for the crown isomer); solid squares are clearing temperatures of the mesophases.

average difference between the two series. Also, there are no conspicuous "even−odd" effects, as often found in such homologous series. The as-synthesized saddle mesogens were obtained in wax form apparently as supercooled mesophases. They did not exhibit clear melting transitions. Likewise, the $n = 5$ crown isomer did not show a melting peak. The enthalpies of the saddle clearing transitions are not given because they could not be accurately determined due to the nearby exothermic peak (see below).

As a typical example we discuss in some details the phase diagrams of the CTV-8 isomers, shown in the upper left part of Figure 5. Trace (a) corresponds to first heating of a virgin sample of the crown isomer. There is a clear melting transition from the solid (K) to the mesophase (M) at 45 °C, followed at 164 °C by a clearing transition to the isotropic liquid (I). The identification of M as a mesophase is based on optical microscopy and X-ray diffraction measurements to be described shortly. These measurements show that M is, in fact, a columnar hexagonal mesophase. Trace (b) corresponds to a virgin sample of the saddle isomer. No clear melting transition is observed, except perhaps for a very broad hump around 45 to 60 °C. The X-ray measurements indicate, however, that above about 50 °C the saddle form is a columnar hexagonal mesophase, with a similar structure as that of the crown. Heating the mesophase leads to an endothermic transition at 137 °C, followed immediately by an exothermic peak (centered at around 142 °C). Further heating leads to a second endothermic peak which falls at exactly the same temperature as the clearing transition of the crown form (164 °C). We interpret this unusual thermogram by the following sequence of transformations: The first endo-

(16) Collet, A.; Dutasta, J.-P.; Lozach, B.; Canceill, J. In *Topics in Current Chemistry*; Weber, E., Ed.; Vol. 165, 1993; 103−129.

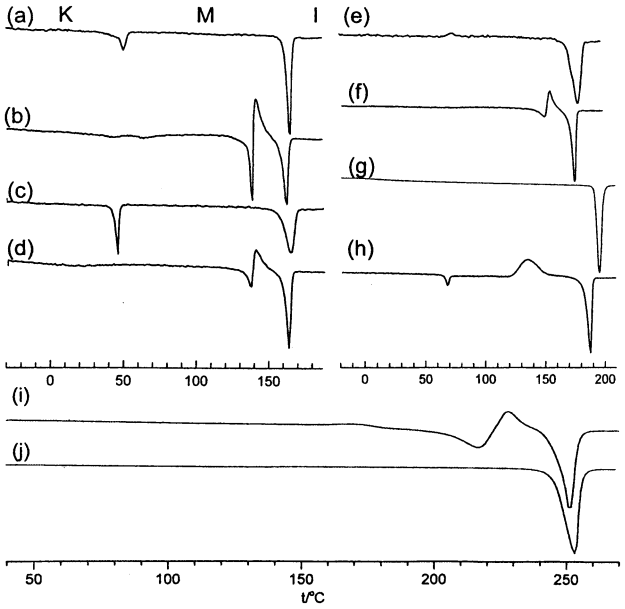


***Figure 5.*** Differential scanning calorimetry (DSC) thermograms of selected homologues of the CTV-*n* series. All experiments correspond to heating at a rate of 10 K/minute. Except for traces (c) and (d), all thermograms correspond to first heating of the as-synthesized material. The symbols K, M, and I are as in Figure 4. (a) $n = 8$, crown; (b) $n = 8$, saddle; (c) $n = 8$, after slow cooling from the melt. (d) $n = 8$, after fast cooling from the melt (e) $n = 4$, crown; (f) $n = 4$, saddle; (g) $n = 3$, crown; (h) $n = 3$, saddle; (i) $n = 2$, crown; and (j) $n = 2$, saddle. Note the reverse behavior of the $n = 2$ isomers (i and j) compared to the other homologues.

thermic transition at 137 °C corresponds to the clearing temperature of the saddle form. In the resulting isotropic liquid, an equilibrium between the crown and saddle forms is established. At this temperature, the isomerization half time is of the order of a few seconds (see Figure 3), so that as soon as liquid is formed, part of the saddle molecules convert to crown. The latter, however, immediately "crystallizes", out of the system to form the more stable crown mesophase, leading to further saddle-crown interconversion until eventually the entire sample is transformed into the crown mesophase. This process is manifested in the exothermic peak at 142 °C. The crown mesophase now remains stable up to its clearing temperature giving rise to the second endothermic transition at 164 °C.

We confirmed this sequence of events by hot-stage optical microscopy combined with $^1$H high-resolution NMR analysis of samples collected during the heating runs. The thermogram of the crown form is straightforward, although the melting transition at 45 °C could not be observed, mainly because the virgin sample was opaque, but the clearing transition was evident. The more interesting behavior is that of the saddle form. The clearing point of its mesophase (137 °C) was clearly detected under the microscope by the appearance of a flowing (dark) isotropic liquid which, however, immediately transformed to a birefringent mesophase. On further heating a second clearing point appears at 164 °C. Several experiments were made in which during the heating, samples were removed from the hot-stage, quenched to room temperature and dissolved in (deuterated) chloroform for $^1$H NMR examination. The spectra of the saddle sample remained unchanged from room temperature up to 137 °C, exhibiting its characteristic fingerprints (see Figure 2). Samples taken between 137 and 164 °C exhibited spectra typical of the crown form, while above 164 °C the spectrum was that of a mixture of both isomers (at a ratio saddle to crown of 0.73 to 0.27).

In traces (c) and (d) of Figure 5 are shown the DSC thermograms of CTV-8 obtained, respectively, after slow cooling (1 °C/min) the isotropic melt through the high-temperature clearing point (164 °C) and following quenching to room temperature. The appearance of the traces is similar to those obtained from the neat crown and neat saddle samples (traces a and b), respectively. These results can readily be understood by the model described above. Slow cooling across the 164 °C clearing point leads to "precipitation" of the crown mesophase out of the melt. The fast isomerization in the supernatant liquid rapidly converts more saddle to crown until the entire sample "crystallizes" as the crown mesophase. On the other hand, when the isotropic liquid is quenched down to room temperature supercooling takes place and when the sample eventually solidifies (or transforms to a supercooled mesophase) the high temperature equilibrium distribution of the isomers is frozen-in, yielding a sample which is predominantly in the saddle form.

Polarizing optical microscopy pictures of the crown mesophase, obtained by slow cooling from the isotropic melt show well-developed spherulites with radial rectilinear defects, similar to those observed for the original pyramidic mesophases[1,2] (see Figure 6). On the other hand, no well-developed domains of the saddle mesophase could be produced in the hot-stage. As mentioned above, the as-synthesized saddle was opaque; fast cooling of the melt yields a mesophase with predominantly the saddle form. However, although birefringent, these specimen resulted in poorly developed domains. The unusual DSC thermogram of the saddle isomer is a consequence of a fortuitous combination of effects. It results from the fact that the compound can exist in two isomeric mesogenic conformations with a wide temperature gap between their clearing points (~30 °C in the present case). Also, the isomerization rate is fast in the melt and extremely slow in the mesophase (and solid states). Under such circumstances, by proper temperature cycling, the compound can be fully transformed to the isomer with the higher clearing temperature (here, crown) or predominantly to the other isomer if it happens to dominate the equilibrium in the melt (as does the saddle form in the present case).

The mesomorphic properties of the CTV-*n* homologues for $n = 5$ to 14 are quite similar to those for CTV-8 and they show similar DSC thermograms. CTV-4 also shows similar behavior, even though the crown form is apparently not mesogenic (while the saddle form is, see Section 3.3 below). The DSC thermograms of the crown and saddle isomers of this homologue are shown as traces (e) and (f) on the top right side of Figure 5. Trace (e) shows a regular melting of the crown solid, whereas trace (f) exhibits an endothermic peak (at 148 °C) due to the clearing of the saddle mesophase, followed by an exothermic crystallization peak (at ~150 °C), yielding solid crown, which then melts at the same temperature as the as-synthesized crown (177 °C).

The CTV-3 isomers are not mesogenic, yet they too exhibit DSC thermograms similar to the higher (mesogenic) homologues. The solid crown (trace g in Figure 5) exhibits a regular melting transition (at 193 °C). The thermogram of the saddle form (trace h) is particularly interesting. Upon heating the as-synthesized solid, it melts (at 67.5 °C) to a flowing isotropic

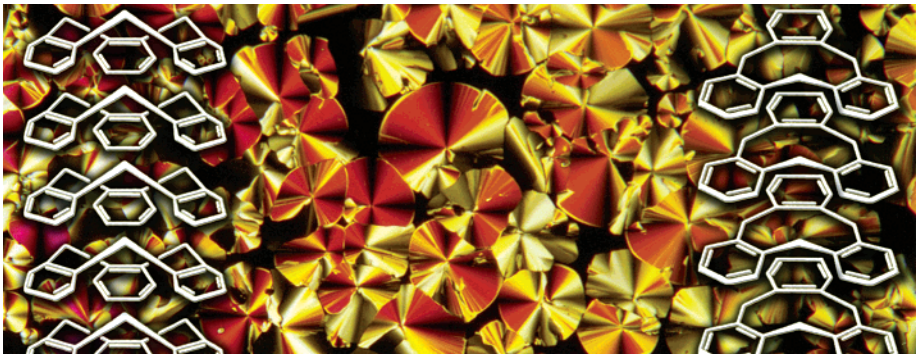

***Figure 6.*** Polarizing optical microscopy picture (×80) of the crown isomer of CTV-8 in the mesophase at 145 °C, obtained by slow cooling (0.2K/min) from the melt. The picture is over-printed (in white) with schematic drawings of the columns in the crown (left) and saddle (right) mesophases

liquid, as observed by polarizing optical microscopy. The liquid soon glassified into an amorphus solid. Upon further heating, it crystallizes exothermically at 134 °C and then melts to the isotropic liquid at 186 °C. $^1$H NMR of samples taken of the solid up to the first melting at 67.5 °C are consistent with a pure saddle form. Above this transition, there is a gradual increase of the crown isomer (13% at 75 °C and 31% at 125 °C), whereas above the 134 °C exothermic peak the sample is entirely in the crown form. X-ray measurements of the latter indicate that it is highly crystalline. Its melting point is slightly lower (at 186 °C) than that of the as-synthesized sample (at 193 °C), perhaps because it is a polymorph of the latter or still contains some amorphous material. In the high-temperature liquid (above 193 °C) an equilibrium mixture containing predominantly saddle (78%) is obtained. We thus have a sequence in which the solid saddle melts to the liquid, but because of the relatively low melting temperature, the isomerization is slow and the crown form appears gradually, on the order of several minutes, rather than immediately as for the other saddle homologues. The slow formation of the crown form results in the glassified saddle-crown mixture, which eventually crystallizes (at 134 °C) in an essentially pure crown form.

Finally, we comment on the CTV-2 homologue. Both isomers are nonmesogenic and their solids are crystalline. Unlike all other members of the series, here the saddle isomer is thermodynamically more stable and melts at a higher temperature than the crown (248 °C as compared to 218 °C, see Table 1 and Figure 4). The DSC thermograms for these compounds are shown as the bottom traces of Figure 5. The saddle form (trace j) shows a single, exceptionally high (248 °C) melting transition. $^1$H NMR measurements of samples taken on heating show no formation of crown up to the melting point. The DSC thermogram of the crown isomer (trace i) shows a completely different behavior. On heating, it exhibits a melting transition at 218 °C, followed immediately by an exothermic transition and on further heating by a second endothermic transition at 248 °C. Unlike in all other homologues, here, the melting of the crown first yields a liquid mixture of crown and saddle from which the latter rapidly crystallizes out until all the material is consumed, leading to a pure saddle solid. This interpretation was confirmed by $^1$H NMR measurements of samples taken during the heating process. Proton NMR measurements of a melt quenched from above 248 °C yielded a saddle/crown ratio of 0.78/0.22. Slow cooling of the melt resulted in pure saddle, albeit in a glass form. Reheating exhibited a glass transition at 117 °C, followed by an exothermic crystallization peak at 223 °C and melting at

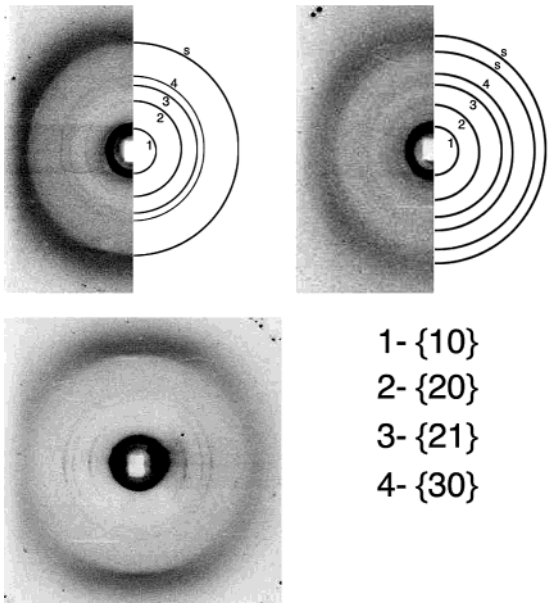


***Figure 7.*** X-ray diffraction patterns of the mesophases of the CTV-8 homologues. Top left: Diffraction pattern of a nonaligned sample of the crown isomer at 91 °C and a graphical representation of the most pronounced sharp diffraction rings. Top right: Analogous presentation for the saddle isomer at 79 °C. The Miller indices for the low-angle rings 1 to 4 (corresponding to two-dimensional hexagonal lattices) are listed at the bottom right of the figure. The weak (but sharp) rings denoted as s correspond to intracolumnar scattering distances, or to 3D diffraction maxima involving these distances. The diffuse outer ring corresponds to scattering from the liquidlike aliphatic chains. Bottom left: Diffraction pattern from an aligned sample of the crown mesophase (at 100 °C), obtained by slow cooling from the melt. Note that the low-angle diffraction arcs 1 to 4 lie predominantly in the horizontal plane, while the s-diffraction maximum is most pronounced in the vertical direction and the diffuse ring is essentially isotropic. The intense spots near the periphery of the diffraction patterns are due to the calcite calibrating material.

248 °C. When the glassy sample was left at room temperature for a day or so, it eventually crystallized. Likewise, when either the saddle or the crown forms were briefly refluxed in high boiling-point liquids (*p*-xylene, at 138 °C and Decalin at 193 °C) and then allowed to slowly crystallize, pure saddle form was always obtained.

**3.3. X-ray Measurements.** The mesophases and solids of several of the CTV-n homologues were investigated by X-ray diffraction. As in the previous section, we provide a rather complete description for the CTV-8 isomers and then fill in some more details on other selected homologues.

In Figure 7 are shown X-ray diffraction patterns for the mesophases of the crown (top left) and saddle (top right) isomers

***Table 2.*** X-ray Diffraction Spacings and Lattice Parameters (*a*) for the Hexagonal Mesophases of the Crown (C) and Saddle (S) Isomers of the CTV-*n* Homologues Studied in the Present Work. All Data Are in Å

| compd | *t*/°C | {10} | {11} | {20} | {21} | {30} | s[a] | a |
|---|---|---|---|---|---|---|---|---|
| CTV-5 (C) | 100 | 17.8 | 10.3 | 8.8 | | | 4.77; 4.42 | 20.4 ± 0.1 |
| CTV-6 (C) | 84 | 18.8 | 10.9 | 9.4 | 7.10 | | 4.76; 4.43 | 21.7 ± 0.0 |
| CTV-8 (C) | 123 | 22.3 | | 11.0 | 8.30 | 7.40 | 4.96 | 25.4 ± 0.2 |
| CTV-9 (C) | 72 | 23.4 | 13.5 | 11.4 | 8.70 | 7.65 | | 26.7 ± 0.2 |
| CTV-14(C) | 90 | 28.3 | 16.5 | 14.0 | | | | 32.6 ± 0.1 |
| CTV-4 (S) | 102 | 15.2 | 8.83 | 7.55 | | | 4.37 | 17.6 ± 0.0 |
| CTV-5 (S) | 120 | 17.6 | 10.2 | 8.87 | 6.72 | | 5.12; 4.90; 4.52; 4.02 | 20.5 ± 0.1 |
| CTV-8 (S) | 76 | 21.3 | | 10.5 | 7.80 | 6.80 | 5.27; 4.78 | 24.0 ± 0.1 |
| CTV-14(S) | 80 | 25.8 | 15.1 | 13.0 | | | | 30.0 ± 0.1 |

[a] Moderately sharp, high angle reflections believed to be associated with intracolumnar stacking.

of CTV-8, recorded at 91 °C and 79 °C, respectively. Also included in the figures are graphical representations of the most pronounced diffractions rings. The patterns for the two isomers are quite similar. They exhibit one strong and three weak sharp (low-angle) rings ($2\Theta < 15°$, corresponding to *d* spacings of more than 6 Å) and a diffuse ring near the outer edge of the pattern (at around 4.5 Å). Such a diffuse ring is often observed[17] in discotic columnar mesophases and is attributed to scattering from disordered aliphatic side chains. The four sharp rings can readily be indexed on a two-dimensional hexagonal lattice with the Miller indices indicated in the figure. The corresponding spacings and lattice parameters for both isomers are summarized in Table 2. Calculation of the surface area indicates that there is one molecule per 2D unit cell.

In Figure 7, we also refer to very weak, but relatively sharp diffraction rings (labeled s) superposing the diffuse ring. They are not as readily apparent as the low angle rings, but they are consistently observed. Just one such ring appears for the crown isomer (corresponding to a spacing of ∼5 Å), whereas there are two in the diffraction pattern of the saddle (at 4.8 Å and 5.3 Å). They are most likely related to the intracolumnar stacking distance. This assignment is supported by a diffraction pattern obtained from a partially aligned sample of the crown mesophase (see Figure 7, bottom left). This sample was prepared by slow cooling of the melt within the (horizontal) magnetic field of the X-ray camera.[14] Instead of diffraction rings we now observe diffraction arcs. Those for the 2D lattice (1 to 4) lie predominantly in the horizontal plane, whereas the arc due to the stacking diffraction is most intense in the vertical direction. The diffuse ring is essentially isotropic with a slight preference for the vertical direction. These results confirm the relationship of the s-ring to the stacking periodicity. At the same time, the experiment also indicates that the preferred alignment of the mesophase is with the director (the direction of the columns) perpendicular to the direction of the magnetic field. Similar magnetic alignment effects have been observed in other pyramidic mesophases.[7] If we assume that the s-peak in the crown mesophase corresponds to the 001 reflection of the hexagonal lattice, its *d* spacing (5 Å) can be identified as the mean intracolumnar distance between the molecules. Its appearance in the X-ray diffraction pattern classifies the mesophase as ordered-hexagonal ($D_{ho}$). The fact that two s-rings appear in the saddle mesophase is puzzling. It may indicate three-dimensional ordering (correlation between neighboring columns) but no complete analysis of the diffraction data of this diffraction pattern was possible.

X-ray diffraction patterns were also obtained for the crown form of the $n = 5$, 6, 9 and 14 homologues and for the saddle isomers of $n = 4$, 5 and 14. In all cases, at least three sharp diffraction rings were observed that could be indexed on two-dimensional hexagonal lattices as for the CTV-8 isomers, as well as a diffuse ring, at approximately 4.5 Å. In some cases, weak, but relatively sharp, wide angle peaks probably associated with intracolumnar stacking, could also be identified. The list of diffraction rings and associated lattice parameters are summarized in Table 2. The lattice constants of the hexagonal mesophases, *a*, for the various compounds studied are also plotted in the upper part of Figure 8 as a function of the number of carbons, *n*, in the side chains. Within each isomeric series, there is roughly a linear relationship between *a* and *n*. Extrapolation to $n = 0$ gives for the crown and saddle series essentially the same value (13.9 Å and 14.2 Å), but the slopes are somewhat different, 1.36 Å and 1.15 Å per $CH_2$ group, respectively. The derived effective size of the unsubstituted core is in good agreement with earlier crystallographic measurements of unsubstituted CTV (crown isomer).[19] The increase in the lateral dimension with increasing *n* is less than expected for a $CH_2$ group in an all-trans conformation, indicating that the side chains are disordered in the mesophase, i.e., folded and/or interdigitated.

The crown isomers of the lower homologues ($n = 5$ and 6) exhibit a pair of weak diffraction rings at *d* values between 4 and 5 Å. As for the saddle mesophase of CTV-8, they could not be indexed on the 2D hexagonal lattices, but indexing on a 3D lattice with stacking distances of 4.8 to 4.9 Å was possible.

The diffraction *d*-spacings for the $n = 8$ crown homologue were also measured as a function of the temperature in the range from 90 to 135 °C. The results, summarized in the lower part of Figure 8, indicate essentially no change in either the stacking, or the lateral spacings. This lack of thermal expansion/contraction effects is somewhat surprising. In columnar discotic[20,21] as well as in thermotropic[22] and lyotropic[23] smectic mesophases, small, but distinct negative thermal expansion coefficients ($\sim 10^{-3}$/K) were detected. The lack of thermal effects in the present system is perhaps due to compensating

(17) Levelut, A.-M. *J. Chim. Phys.* **1983**, *80*, 149−161.
(18) Spielberg, N.; Sarkar, M.; Luz, Z.; Poupko R.; Zimmermann, H. *Liq. Cryst.* **1993**, *15*, 311−330.
(19) Hyatt, J. A.; Duesler, E. N.; Curtin, D. Y.; Paul, I. C. *J. Org. Chem.* **1980**, *45*, 5074−5079.
(20) Zamir, S.; Singer, D.; Spielberg, N.; Wachtel, E. J.; Zimmermann, H.; Poupko, R.; Luz, Z. *Liq. Cryst.* **1996**, *21*, 39−50.
(21) Fontes, E.; Heiney, P. A.; de Jeu, W. H. *Phys. Rev. Lett.* **1988**, *61*, 1202−1205.
(22) Budig, H.; Diele, S.; Goring, P.; Paschker, R.; Sauer, C.; Tschierske, C. *J. Chem. Soc., Perkin Trans.* **1995**, *2*, 767−775.
(23) Nagle, J. F.; Zhang, R. T.; Tristram-Nagle, S.; Sun, W. J.; Petrache, H. I.; Suter, R. M. *Biophys. J.* **1996**, *70*, 1419−1431.

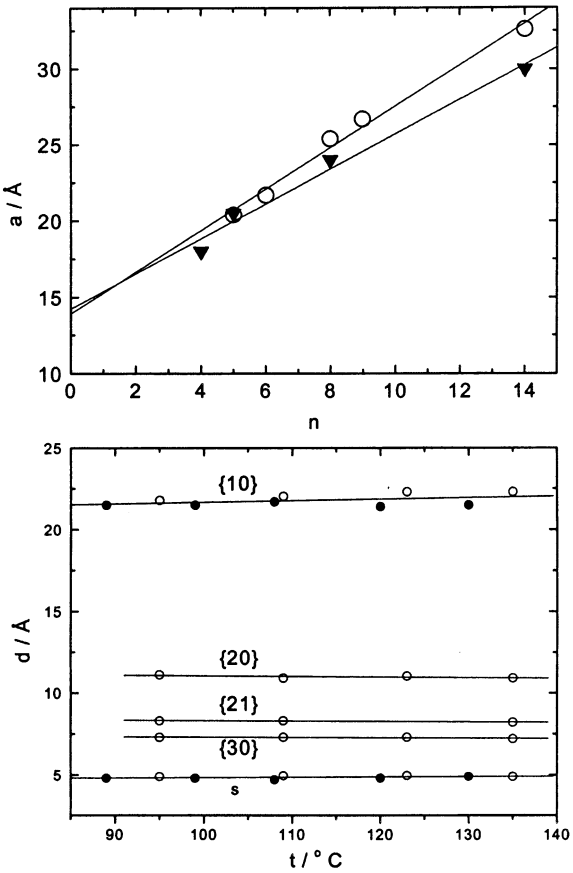


***Figure 8.*** Top: Plots of the hexagonal lattice constant for the mesophases of the crown (open circles) and saddle (solid triangles) isomers as a function of the number of carbons in the side chains. Bottom: The *d* spacings of the indicated X-ray diffraction maxima for the crown isomer of CTV-8 as a function of the temperature within the mesophase region. The solid and open symbols correspond, respectively, to measurements taken upon heating from room temperature and cooling from the melt.

tendencies, thermal expansion, and increase in chain disorder, allowing closer contact between the molecules.

All the crown mesogens, except the $n = 5$ homologue, exhibited a clear first-order DSC peak on heating the virgin samples from room temperature to the mesophase region. In general these transition temperatures increase with increasing n, and except for the $n = 13$ homologue they exhibit a mild even−odd alteration (see Table 1 and Figure 4). The X-ray structure of the phases underlying the hexagonal mesophase was studied at room temperature for the $n = 5$, 6, 8, 9, and 14 homologues. Most of them exhibit a diffuse ring at ∼4.5 Å and a maximum of nine diffraction rings for *d*-spacings larger than 4 Å. The low angle diffraction of the $n = 5$ and 6 homologues was similar to that of the corresponding hexagonal phases. The intermediate homologues ($n = 8$, 9), displayed quite different patterns, but we were unable to index them. On the other hand, the pattern of the CTV-14 could be interpreted in terms of a 2D rectangular lattice (with $a = 45.6$ Å, $b = 35.5$ Å). It thus appears that the phases underlying the hexagonal mesophases of the crown series are at most disordered solids and perhaps some of them, more ordered discotic mesophases.

As indicated above, no melting transition into the mesophase upon heating the as-synthesized saddle samples was observed. In fact X-ray measurements performed at room temperature on the $n = 4$, 5, 8, and 14 homologues gave similar diffraction

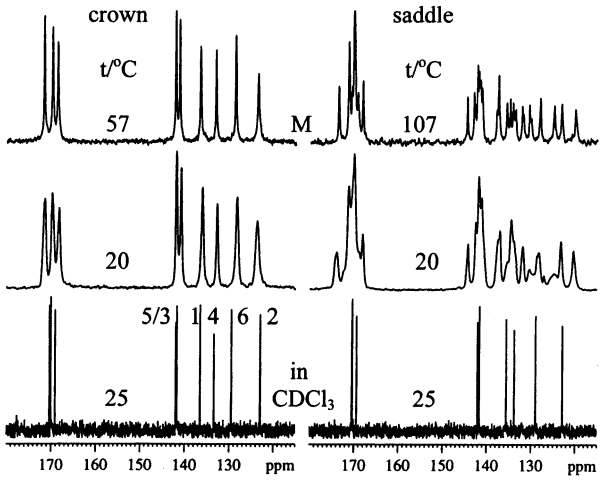


***Figure 9.*** Carbon-13 NMR spectra of the crown (left) and saddle (right) isomers of CTV-8. Only the low field range, featuring the aromatic and carboxylic signals, are shown. The bottom traces are for isotropic solutions in $CDCl_3$ at room temperature. The peak assignment in the crown spectrum is according to the numbering system in Figure 1(b). The same assignment applies to the saddle isomer. The middle traces are CPMAS spectra of neat samples recorded at room temperature. They correspond to the solids and supercooled mesophases of the crown and saddle isomers, respectively. The top traces are of the mesophases recorded at the indicated temperatures. The MAS spectra were recorded at a spinning rate of 5 kHz; recycle time 5 to 10 s and the number of scans varied from 160 to 600.

patterns to those of the corresponding hexagonal mesophases at higher temperature. Only for CTV-8 were we unable to index the room-temperature diffraction pattern. It is thus possible that, with the exception of the latter, the hexagonal mesophases of the saddle isomers extend (or supercool) down to room temperature and below.

The crown and saddle homologues with $n = 2$ and 3, as well as the crown of $n = 4$, are not mesogenic. The room temperature X-ray diffraction of the virgin crown and saddle CTV-2 isomers are characteristic of crystalline materials, but with different structures. On cooling from the melt, pure saddle is obtained, but in a glassy state, which crystallizes after a day or so at room temperature. The as-synthesized $n = 3$ saddle compound appeared to be a disordered solid, exhibiting 3 or 4 broad rings. After melting, the liquid gradually solidifies as the crown isomer (see Section 3.2 above). As indicated above, this material is amorphous but crystallizes above 134 °C exhibiting solid-like diffraction rings. The $n = 4$ crown is crystalline, exhibiting 5 diffraction rings with spotty textures. These rings can, in fact, be indexed on a two-dimensional hexagonal lattice with $a = 18.6$ Å. There are also high angle rings (at $d = 4.61$ Å and 4.31 Å), but no diffuse ring corresponding to molten side chains.

## 4. Carbon-13 NMR and Dynamic Properties of the Mesophases

**4.1. High-Resolution Solution Spectra.** Carbon-13 MAS NMR measurements were performed on the crown and saddle isomers of selected homologues of the CTV series to study their dynamic properties in the mesophase. The most extensive measurements were performed on the $n = 8$ homologue. Examples of carbon-13 spectra for the crown and saddle isomers of this homologue are shown on the left and right-hand sides of Figure 9, respectively.

Before discussing the MAS spectra, we briefly comment on the high-resolution solution spectra (in chloroform) shown at

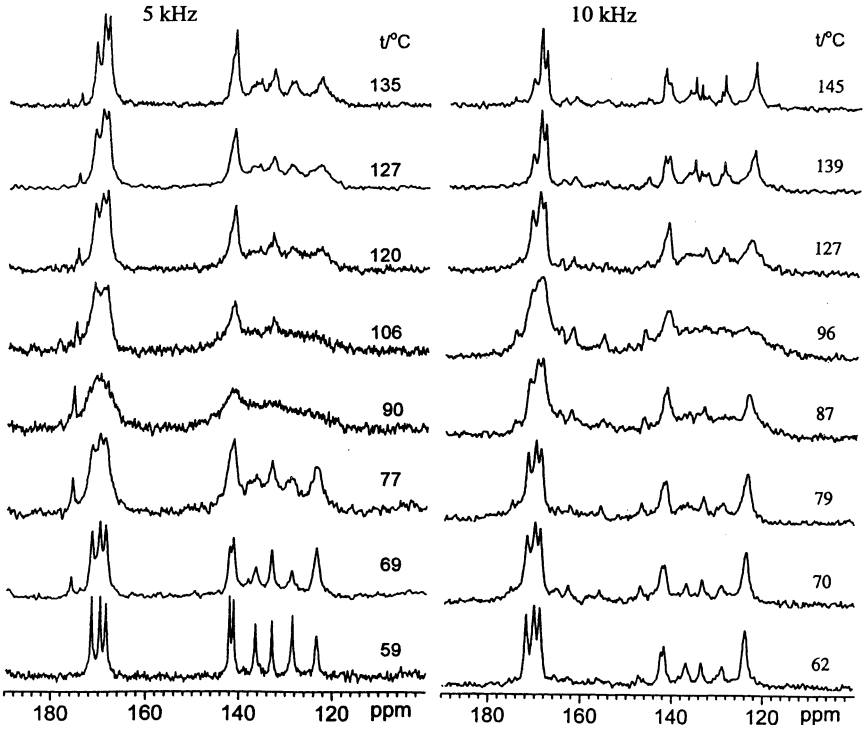


***Figure 10.*** Carbon-13 MAS spectra of the crown isomer of CTV-8 within the mesophase as a function of the temperature at two spinning rates, as indicated (5 kHz on the left and 10 kHz on the right). Only the low field region of the aromatic and carboxylic carbons is shown. Except for the bottom trace at 5 kHz, which was recorded by CP, all other spectra were obtained by single pulse excitation. Recycle times ranged from 5 s (at low temperatures) to 3 s (at higher temperatures). The numbers of scans ranged from 100 to 10 000 depending on the line widths. The sharp signal at 174 ppm observed in some of the spectra (where the line broadening is more pronounced) is due to a small amount of the saddle isomer present in the sample.

the bottom traces in the figure. Only the low-field regions featuring the carboxylic and aromatic carbons are shown. Those due to the aliphatic carbons fall in the range from 14 to 35 ppm. We shall not be concerned with these signals, except to mention the chemical shift (CS) ranges of the carbons due to the end methyls (14 to 15 ppm), the chain α-methylenes (∼34 ppm) and the ring-methylenes (29 ppm). The signals due to the aromatic (122 to 143 ppm) and carboxylic (168 to 172 ppm) carbons (Figure 9) are well separated, and the latter could readily be identified (except for the closely spaced carbons 3 and 5) on the basis of CS additivity rules.[24] The C−H peak at 123 ppm was also directly assigned on the basis of carbon−hydrogen correlation spectroscopy and the appearance of a doublet in the solution spectra in the absence of decoupling. The assignment is indicated for the solution crown spectrum in Figure 9 using the numbering system given in Figure 1b and is the same for the saddle spectrum. The actual CS values are given in Tables 3,A and B, respectively. The solution spectrum of the crown isomer with six aromatic and three carboxylic peaks is consistent with its rigid $C_3$-symmetry structure. The room-temperature solution spectrum of the saddle form is very similar to that of the crown. However, in this case, it reflects the averaging over the various saddle conformations due to fast pseudorotation (Figure 1f), leading to an average $C_{3h}$ symmetry.

**4.2. Crown Isomer of CTV-8 in the Solid and Mesophase.** Carbon-13 MAS spectra of the crown form of CTV-8 in the solid (room temperature) and mesophase are shown (aromatic and carboxylic regions only) in the center and top traces of the left column of Figure 9. The general features of these spectra are quite similar to each other and to that of the solution (bottom trace), allowing easy correlation of the peaks in the different traces. The spectra in the solid/mesophase also exhibit spinning sidebands (ssb), reflecting the large CS anisotropy of the various nuclei. The ssb are not shown in the figure; however, for subsequent discussion, we have analyzed the solid-state spectrum in terms of the full chemical shift tensors of the aromatic and carboxylic carbons. For the quantitative analysis, we used spectra recorded at several low spinning rates (1.8 to 3.9 kHz) and applied the Herzfeld-Berger formalism[25] and subsequent refinement by comparison with calculated spectra. The results are summarized in Table 3(A). The assignment of the peaks in this table is according to the numbering system in Figure 1b. The resulting CS anisotropies are consistent with literature data.[26]

The spectrum for the crown mesophase shown in Figure 9 was recorded at the low-temperature range of its stability range (57 °C). On heating, the sample within the mesophase region, linebroadening sets-in, resulting in excessive line overlap between neighboring peaks. Eventually, the lines narrow again with essentially no change in their positions. Examples of spectra showing the effect are depicted in Figure 10. Two sets of spectra, recorded at spinning rates of 5 and 10 kHz by single pulse excitation (rather than CP) are shown. The behavior clearly indicates the setting-in of a dynamic effect on the NMR time scale. It is natural to associate this effect with molecular 3-fold jumps about the column axes. Support for this model comes from a two-dimensional MAS exchange experiment the results

(24) Kalinowski, H. A.; Berger, S.; Braun, S. In *Carbon-13 NMR Spectroscopy*, Wiley: New York, 1988; Chapter 3.

(25) Herzfeld, J.; Berger, A. F. *J. Chem Phys.* **1980**, *73*, 6021−6030.

(26) Duncan, T. M. *Principal Components of Chemical Shift Tensors: A Compilation*, 2nd ed.; The Farragut Press: Madison, 1997.

***Table 3.*** Carbon-13 Chemical Shift Parameters (in ppm) for the Aromatic and Carboxyl Carbons of the CTV-8 Isomers

(A) results for the crown form derived from MAS spectra recorded at 40 °C

| assignment[a] | $\delta_{iso}$ | $\delta_{11}$ | $\delta_{22}$ | $\delta_{33}$ | $\delta_{iso}$(solution) |
|---|---|---|---|---|---|
| C−H(2) | 123.6 | 80 | 20 | −100 | 123.0 |
| C−C(6) | 128.6 | 75 | 27 | −102 | 129.5 |
| C−O(4) | 133.1 | 61 | 5 | −66 | 133.4 |
| C−C(1) | 136.5 | 85 | 27 | −112 | 136.5 |
| C−O(3/5) | 141.2 | 72 | −6 | −66 | 141.7 |
| C−O(5/3) | 142.1 | 77 | −2 | −75 | 142.0 |
| C(O)O(7) | 168.5 | | | | 169.1 |
| C(O)O(8) | 169.8 | 91 | −41 | −50 | 170.1 |
| C(O)O(9) | 171.6 | | | | 170.4 |

(B) results for the aromatic carbons in the saddle form derived from the mesophase spectrum at 77 °C. The peak labeling is as in Figure 13.

| peak no. | assignment | $\delta_{iso}$ | $\delta_{11}$ | $\delta_{22}$ | $\delta_{33}$ | $\nabla/10^4$ Hz$^2$ | $\langle\delta_{iso}\rangle$ | $\delta_{iso}$(solution) |
|---|---|---|---|---|---|---|---|---|
| a | | 120.2 | 78 | 8 | −86 | | | |
| b | C−H(2) | 123.3 | 82 | 8 | −90 | 3.72 | 122.8 | 122.9 |
| c | | 124.8 | 87 | 12 | −99 | | | |
| d | | 128.1 | 75 | 33 | −108 | | | |
| e | C−C(6) | 130.7 | 79 | 28 | −107 | 2.91 | 130.3 | 128.9 |
| f | | 132.2 | 69 | 38 | −107 | | | |
| g | | 133.6 | | | | | | |
| h | C−O(4) | 134.4 | 64 | −7 | −57 | 0.76 | 134.6 | 133.7 |
| j | | 135.7 | | | | | | |
| i | | 134.9 | | | | | | |
| k | C−C(1) | 137.4 | | | | 1.74 | 136.7 | 135.5 |
| l | | 137.9 | 90 | 31 | −121 | | | |
| m | | 141.2 | | | | | | |
| n | C−O(3/5) | 141.5 | 81 | −11 | −70 | 0.08 | 141.5 | 141.6 |
| o | | 141.9 | | | | | | |
| p | | 142.2 | | | | | | |
| q | C−O(5/3) | 143.0 | | | | 0.92 | 143.2 | 142.0 |
| r | | 144.5 | 77 | −5 | −72 | | | |

(C) results for the carboxylic carbons in the saddle form derived from the mesophase spectrum at 77 °C.

| peak no.[b] | assignment | $\delta_{iso}$ | $\delta_{i11}$ | $\delta_{22}$ | $\delta_{33}$ | $\nabla/10^4$ Hz$^2$ | $\langle\delta_{iso}\rangle$ | $\delta_{iso}$(solution) |
|---|---|---|---|---|---|---|---|---|
| s(1) | | 168.1 | | | | | | |
| v(1) | C(O)O | 170.7 | | | | 5.50 | 170.9 | $170.3_7$ |
| x(1) | | 173.8 | | | | | | |
| t(1) | C(O)O | 169.3 | | | | | 170.7 | $170.4_4$ |
| w(2) | | 171.4 | | | | 0.98 | | |
| u(3) | C(O)O | 170.2 | 92 | −46 | −46 | 0 | 170.2 | 169.4 |

[a] The labeling (assignments) of the aromatic carbons refers to the numerical system in Figure 1b. The labeling of the carboxylic carbons is not related to the molecular structure. The $\delta_{iso}$(Solution) were measured in chloroform solutions. All other results refer to the solid/mesophases and were determined from MAS NMR spectra. The $\delta_{iso}$ are relative to TMS. The $\delta_{kk}$ are principal values relative to their respective $\delta_{iso}$, so that $\sum\delta_{kk} = 0$ and $\delta_{11} > \delta_{22} > \delta_{33}$. The $\langle\delta_{iso}\rangle$ (for the saddle form) are averages over triplets of $\delta_{iso}$'s and the $\nabla$'s are their second moments (in units of 10 $^4$Hz$^2$) calculated for $\nu_L = 100$ MHz as explained in the text. [b] The numbers in bracket are approximate relative intensities of the peaks (see top left spectrum in Figure 13).

of which is shown on the left-hand side of Figure 11. The spectrum was recorded at 61 °C, just before the line broadening becomes significant, using the method of Veeman and co-workers.[27] The mixing period was $\tau_m = 1$ s, the spinning frequency, $\nu_R = 4.2$ kHz and the spectrum magnitude is plotted. In such experiments dynamic processes are manifested by the appearance of off-diagonal cross-peaks in the 2D spectrum. Cross-peaks linking peaks belonging to different ssb manifolds (hetero cross-peaks)[28] indicate exchange between inequivalent carbons (chemical exchange). On the other hand, cross-peaks linking ssb of the same manifold (auto cross-peaks) indicate a pure (physical) reorientation process. Referring to Figure 11 and the 1D spectrum displayed at its top, it may be seen that each of the aromatic and carboxylic center band signals exhibits auto cross-peaks with at least two ssb on each side, resulting in strings of cross-peaks parallel to the main diagonal. This clearly indicates the presence of a pure reorientation process, as would be expected for 3-fold jumps. This interpretation is also supported by the general appearance of the 1D spectra in Figure 10. In particular, it may be seen that the signals with the smallest CS anisotropy are least broadened (see, for example, the aromatic C−O peaks at 133 and 142 ppm) and that the maximum broadening is smaller for the spectra recorded at 10 kHz compared to those recorded at 5 kHz.

For the determination of the kinetic parameters of this process, we performed a quantitative analysis of 1D spectra of the type shown in Figure 10. To do so, we compared these experimental spectra with simulated ones as described below. For the detailed analysis, we selected the center-band signal of the aromatic C−H carbon (at 123.6 ppm) because its assignment is most certain, it is well separated from the rest of the peaks and thus suffers least from overlap effects and because for this carbon the directions of the principal components of the CS tensor can best be guessed. Although the principal values of all the aromatic carbons could be determined from the analysis of the ssb (see

(27) de Jong, A. F.; Kentgens, A. P. M.; Veeman, W. S. *Chem. Phys. Lett.* **1984**, *109*, 337−342.
(28) Luz, Z.; Spiess, H. W.; Titman, J. J. *Israel J. Chem.* **1992**, *32*, 145−160.

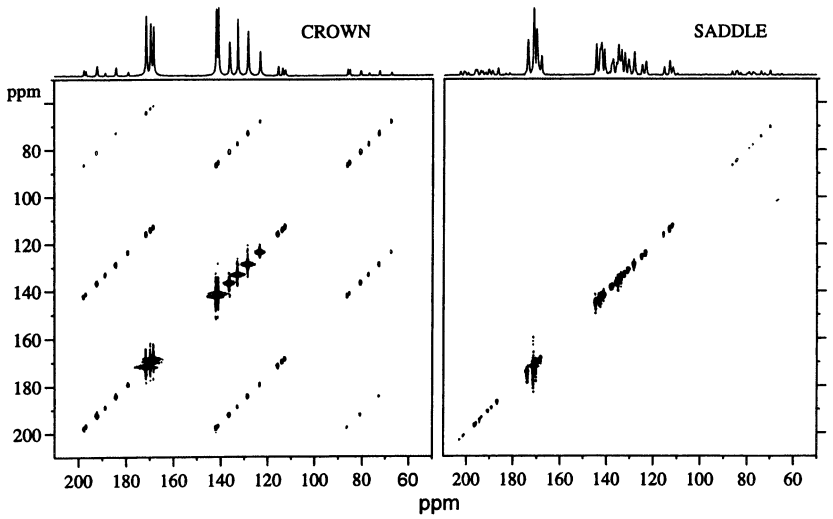


***Figure 11.*** Carbon-13 rotor synchronized 2D exchange spectra for the crown (left) and saddle (right) isomers of CTV-8 in the mesophase region. One-dimensional projection spectra, including two sets of spinning sidebands are depicted at the top. Experimental details for the crown: temperature, 61 °C; spinning rate, 4.2 kHz; mixing time, 1 s; recycle time, 2 s; CP contact time, 2 ms; number of $t_1$ increments, 256, 60.6 $\mu$s apart, 100 scans each; dwell time in the $t_2$ domain, 30.3 $\mu$ s; total number of acquisition points, 2000. Corresponding details for the saddle isomer: 80 °C; 4.4 kHz; 10 s; 2 s; 3 ms; 300 $t_1$ increments, 55.6 $\mu$s apart, 50 scans each; $t_2$ dwell time, 27.8 $\mu$s: 2000 acquisition points.

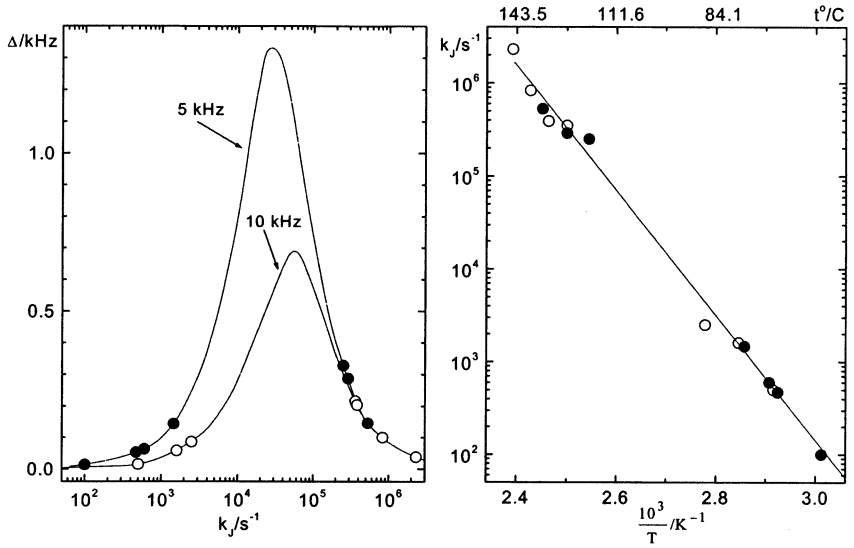


***Figure 12.*** Left: Calculated line width (full width at half-maximum height) in the carbon-13 MAS spectra for the center band of the aromatic C−H carbon (#2) as a function of the 3-fold jump rate, for spinning frequencies of 5.0 and 10 kHz, as indicated. The plots were calculated as explained in the text and correspond to a natural line width, $1/T_2^\circ = 0$. The open and solid symbols correspond to experimental exchange induced line widths measured from spectra of the type shown in Figure 11. Right: Arrhenius plot for the 3-fold jump rate in the mesophase of the crown form of CTV-8. The open and solid symbols correspond to experimental results obtained at 5 and 10 kHz, respectively.

Table 3), the principal directions must be inferred from the molecular structure. This is least problematic for the C−H carbon. On the basis of earlier measurements, it is quite safe to associate the principal values for this carbon with its local symmetry axes.[29−31] Thus, we set the most shielded value to lie normal to the benzene ring ($\delta_{33} = -100$ ppm) and the least shielded one to lie along the C−H bond direction ($\delta_{11} = 80$ ppm), so that the intermediate principal value ($\delta_{22} = 20$ ppm) lies in the plane of the benzene ring perpendicular to the C−H bond direction. The angle between the molecular $C_3$ axis and the normal to the benzene plane was taken as 43°.[6]

For the simulations of the dynamic MAS spectra of the C−H carbon, we used the Floquet method,[32,33] with the CS and geometrical parameters described above. The computations were made for a fixed natural line width of $1/\pi T_2^\circ = 100$ Hz. The spectra of the center band were then displayed, their full width at half-maximum intensity measured and the fixed natural width, $1/\pi T_2^\circ$, was subtracted, thus yielding the dynamic line width parameter, $\Delta$. This parameter is plotted on the left-hand side of Figure 12 as a function of the rate, $k_J$, of the 3-fold jumps for the two spinning frequencies used experimentally (10 and 5 kHz). To derive rate constants from the experimental spectra the full width at half-maximum height of the C−H peak was measured and an appropriate natural line width was subtracted

(29) Pausak, S.; Pines, A.; Waugh, J. S. *J. Chem. Phys.* **1973**, *59*, 591−595.
(30) van Dongen Torman, J.; Veeman, W. S. *J. Chem. Phys.* **1978**, *68*, 3233−3235.
(31) Carter, C. M.; Facelli, J. C.; Alderman, D. W.; Grant, D. M.; Dalley, N. K.; Wilson, B. E. *J. Chem. Soc. Faraday Trans. 1*, **1988**, *84*, 3673−3690.
(32) Schmidt, A.; Vega, S. *J. Chem. Phys.* **1987**, *87*, 6895−6907.
(33) Luz, Z.; Poupko, R.; Alexander, S. *J. Chem. Phys.* **1993**, *99*, 7544−7553.

to yield an experimental dynamic width, Δ. Comparison with the calibration plots in Figure 12 finally yielded $k_J$. The choice of the fast and slow exchange branches in the calibration curves is obvious from the temperature dependence of the spectra (Figure 10). The measured Δ's used to derive the rate constants are indicated on the calibration curves (solid and open symbols for 5 and 10 kHz, respectively) and the results for $k_J$ are plotted on the right-hand side of Figure 12 as a function of the inverse absolute temperature. In practice, results could only be obtained in the slow exchange regime (below ~90 °C) and in the fast exchange regime (above ~120 °C) because in the intermediate range, excessive overlap between lines prevented accurate line width measurements. The experimental $1/\pi T_2°$ parameter used in the analysis was 30 Hz for both spinning frequencies in the fast exchange regime and 40/77 Hz, for the 5/10 kHz experiments in the slow exchange range. The larger broadening in the 10 kHz experiments was traced back to a slight misadjustment of the magic angle. It is remarkable that the results derived from the two sets of measurements (10 kHz and 5 kHz) are essentially in complete agreement.

The kinetic parameters for the 3-fold jump process derived from the Arrhenius plot in Figure 12 are

$$k_J = Ae^{-E_a/RT} \text{ with } log\ A(s^{-1}) = 22.49 \pm 0.79,$$
$$E_a = 130.1 \pm 5.8 \text{ kJ/mol}$$

These results are quite unusual. The preexponential factor is orders of magnitude higher than normally obtained or expected from theory and the activation energy is unusually high for molecular reorientation in a mesophase. Similarly extreme values were obtained for the 3-fold jump process in the columnar mesophases of hexa-alkanoyloxy CTV (R′═H, R═OC(O)-$C_{n-1}H_{2n-1}$).[7] Measurements performed by deuterium NMR for the $n$ = 13, 14, and 15 homologues of this series gave the following average values, $A = 7.0 \times 10^{22}$ $s^{-1}$and $E_a$ = 126.4 kJ/mol. As suggested by J. D. Dunitz in connection with another system,[34] unusually high values of $A$ and $E_a$ may result from a decrease of the activation barrier with increasing temperature. For the present system, this could be interpreted as softening of the stacking within the columns with increasing temperature. This could manifest itself also as thermal expansion of the columns. However, as shown in Section 3.3, this does not seem to be the case. No thermal expansion in either the hexagonal lattice parameter, or the stacking distance was detected in the X-ray measurements.

The carbon-13 MAS spectra of a few other crown CTV-$n$ compounds were recorded in the mesophase region, including the $n$ = 5 and 14 homologues. These were not studied inasmuch detailed as the crown CTV-8, nevertheless, an idea about the trend within the series could be obtained from these preliminary observations. No line broadening was observed in the MAS spectra of CTV-5 in the mesophase up to 135 °C, whereas for the CTV-14 the lines were already very broad at the transition to the mesophase (71 °C). Thus, it appears that the 3-fold jump rate increases with increasing length of the side chains. Preliminary deuterium NMR measurements in the mesophase region of the $n$ = 6, 9, and 14 crown homologues, deuterated in the unsubstituted aromatic site, showed a similar trend.

(34) Müller, A.; Haeberlen, U.; Zimmermann, H.; Poupko, R.; Luz, Z. *Mol. Phys.* **1994**, *81*, 1239−1258.

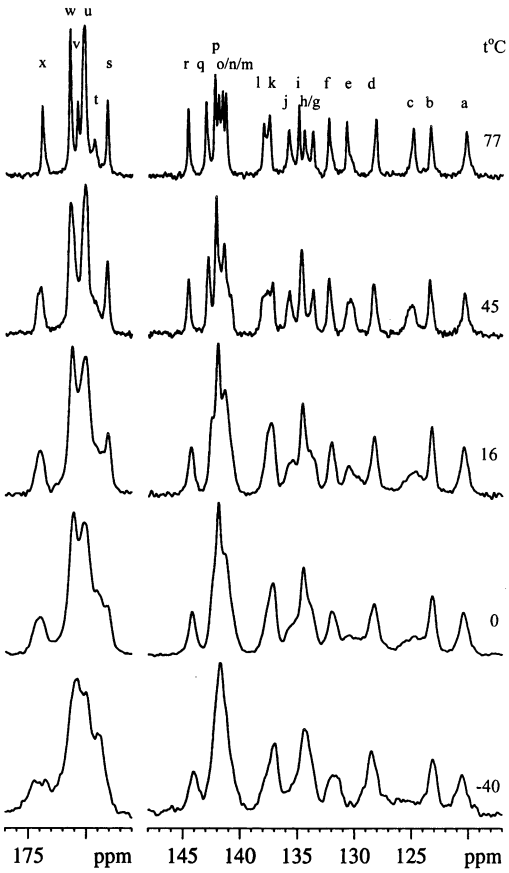


***Figure 13.*** Carbon-13 CPMAS spectra (low-field region only) of the saddle form of CTV-8 in the mesophase as a function of the temperature as indicated. Spinning rate, 5 kHz; recycle time, 5 to 10 s; number of scans, 200 to 1200. At 77 °C, the resolved peaks are labeled alphabetically from high to low field. The assignment of the peaks is discussed in the text and given in Table 3, parts B and C.

**4.3. Saddle Isomer of CTV-8 in the Mesophase.** Carbon-13 MAS spectra of the saddle form of CTV-8 at room temperature and 107 °C are shown on the right-hand side of Figure 9. Expanded spectra with labeling of the peaks are also shown in Figure 13.

At 77 °C, the spectrum clearly exhibits eighteen resolved aromatic peaks, which is exactly the number of inequivalent aromatic carbons in a single saddle conformation of the CTV core. Hence, we conclude that in the solid and mesophase the saddle form is frozen in one conformation and (NMR wise) does not pseudorotate. Under these conditions nine carboxyl peaks are expected. Only six are actually resolved, but with different relative intensities. MAS spectra (recorded at 77 °C with different spinning rates) were subjected to a Herzfeld−Berger analysis[25] and the resulting CS tensors are summarized in Table 3B for the aromatic carbons and in Table 3C for one of the carboxyl carbons. In these tables, the peaks are listed sequentially (alphabetically) in order of increasing $\delta^{iso}$. In practice, because of resolution difficulties, the full tensors were only determined for the aromatic peaks, a−f, h, l, r and the group m/n/o. For the carboxylic carbons, only the strong peak, u, was analyzed. From the CS anisotropies, comparison with $\delta_{iso}$ (solution) and from the structure of the spectrum (peak intensities) we were able to divide the eighteen aromatic lines into groups of triplets and associate each group with a particular type of carbon, as indicated in Table 3B. The assignment was

based on the assumption that the average $\langle\delta_{iso}\rangle$ for each triplet matches as close as possible the $\delta_{iso}$(solution) of a particular carbon in the room-temperature solution spectrum. It was also assumed that carbons of the same type will have similar CP efficiency and therefore similar intensities. For example, consider peaks a, b, c, assigned to the three (inequivalent) aromatic C−H carbons in the saddle conformer. In solution, where pseudorotation is fast, their average isotropic shift is $\delta_{iso}$(solution) = 122.9 ppm, which matches perfectly well the average shift, $\langle\delta_{iso}\rangle$ = 122.8 ppm, obtained by averaging the $\delta_{iso}$ of these peaks in the mesophase. Likewise, we could group all other peaks to sets of triplets, with deviations between $\langle\delta_{iso}\rangle$ and $\delta_{iso}$(solution) not exceeding 1.5 ppm (see Table 3B). Note that, on the basis of the above considerations, we grouped the triplets, g, h, j, and i, k, l, (rather than sequentially, g, h, i, and j, k, l,) matching them with, respectively, peaks 3 and 4 of the isotropic spectrum. All other groupings are quite straightforward. The resolution of the carboxylic peaks is not sufficient to perform a similar complete assignment. On the basis of their relative intensities peaks s, v, x, with $\langle\delta_{iso}\rangle$=171.1 ppm, were assigned to one type of carboxylic carbons, peaks t and w, with intensity ratio 1:2 and $\langle\delta_{iso}\rangle$=170.7 ppm, were assigned to a second type and the strong peak, u, at $\delta_{iso}$=170.2 ppm to a third type of carboxylic group. The range of the $\langle\delta_{iso}\rangle$'s and $\delta_{iso}$'s is too small to allow their identification with the different side chains, or even to correlate between the solution and mesophase spectra.

On heating the saddle sample from about 70 °C, the spectrum remains essentially unchanged up to the clearing temperature. This indicates that the saddle conformation is frozen-in and no rotation or pseudorotation takes place in the mesophase over its entire range of stability. This is also confirmed by the 2D MAS exchange experiment depicted on the right-hand side of Figure 11. The spectrum shown in this figure was recorded at 80 °C, well within the mesophase region, with a mixing time as long as 10 s. Yet no cross-peaks are observed. This result is somewhat surprising in view of the analogous situation in the columnar mesophases of octa-alkyloxy-orthocyclophane (cyclotetra-veratrylene). The core of these discotic molecules consists of the four benzene rings forming a sofa conformation analogous to the saddle form of CTV. In solution, the sofa form is highly flexible, undergoing pseudorotation, much like the saddle form of CTV. In the mesophase the sofa molecules stack on top of each other to form columnar structures. Deuterium (1D and 2D) NMR measurements showed,[35] that in these mesophases reorientation takes place, involving simultaneous pseudorotation and whole molecule rotation. A similar combined process might have been anticipated for the mesophases of the saddle CTV-n homologues. However, the packing of the saddle is apparently too tight to allow such a reaction to take place. The lack of dynamic effects on the carbon-13 NMR spectra of saddle-based mesophases was confirmed by measurements on a few other homologues of the series including the $n$ = 5 and 14 ones.

Referring again to Figures 9 and 13, we note that on cooling the saddle mesophase from 77 °C, there is a general line broadening and some of the peaks also undergo small shifts. Close examination of the aromatic region shows that the broadening is selective, with some of the lines broaden more than others. Conspicuous examples are peaks c of the C−H triplet and e of the first C−C triplet. Less obvious examples are peaks l and m. It appears, however, that at most, one line of each triplet undergoes excess broadening, and it is natural to associate them with the same benzene ring of the saddle core.

This broadening most likely reflects the slowing down of some fast local motion. It is likely that at high temperatures in the mesophase the saddle molecules undergo fast high amplitude local librations, not involving pseudorotation. As the temperature is lowered to below 70 °C, these motions gradually freeze out, leading to a static orientational disorder. This disorder results in a dispersion of the isotropic CS and is responsible for the observed inhomogeneous broadening. Apparently, one of the benzene rings undergoes a larger librational amplitude than the other two ending up in a wider range of static disorder. This conclusion is supported by measurements at different spinning rates. We have performed such measurements at 45 °C, with spinning rates between 2.3 and 10 kHz and no effect on the line width was detected. If the broadening where due to discrete jumps between, say, two twisted saddle conformations differing mainly in their anisotropic CS, the broadening would be expected to depend on the spinning rate. In general, the carboxyl carbons show a similar behavior, but as for the assignment, the resolution is not sufficient for a detailed analysis.

**4.4. Saddle-Crown Interconversion in the Mesophase.** Finally, we comment on the long-term stability of the saddle mesophase. When left for long periods at sufficiently high temperatures the saddle mesophase gradually transforms to the crown mesophase. The process was quantitatively studied on several specimens of CTV-8. Samples of the saddle isomer in the mesophase state were kept at constant temperatures for several hours/days. At preselected times, the samples were quenched to room temperature, dissolved in chloroform and using $^1$H high-resolution NMR the extent of transformation from saddle to crown was determined. At 90 °C, the transformation was found to be quite slow, reaching 10% crown after 48 h. Over the same period, the crown fraction reached 40% at 100 °C and 90% at 110 °C. Recalling that, at equilibrium, in solution the crown form is only 40% at 110 °C (see Figure 3) the almost complete transformation at this temperature reflects the higher thermodynamic stability of the crown compared to the saddle mesophase. Similar qualitative observations were also made on the CTV-5 and CTV-14 saddle homologues. It appears that the transformation is somewhat slower for the shorter homologue and a bit faster for the longer one.

One possible mechanism for the transformation may involve sublimation. The vapor pressure over the less stable saddle mesophase is relatively high. In the vapor phase, there is fast saddle-crown isomerization followed by condensation of the crown mesophase with the lower vapor pressure. Alternatively, the transformation process may be assumed to take place at the glass interface, in structural defects or at domain boundaries, where thermal equilibration between the isomers is more readily established.

## 5. Low-Temperature Carbon-13 NMR of the Saddle Isomer in Solution and Pseudorotation

We expect that at sufficiently low temperatures the pseudorotation of the saddle conformation will freeze out and accordingly affect its NMR spectrum. In contrast, no effects

(35) Kuebler, S. C.; Boeffel, C.; Spiess, H. W. *Liq. Cryst.* **1995**, *18*, 309−318.

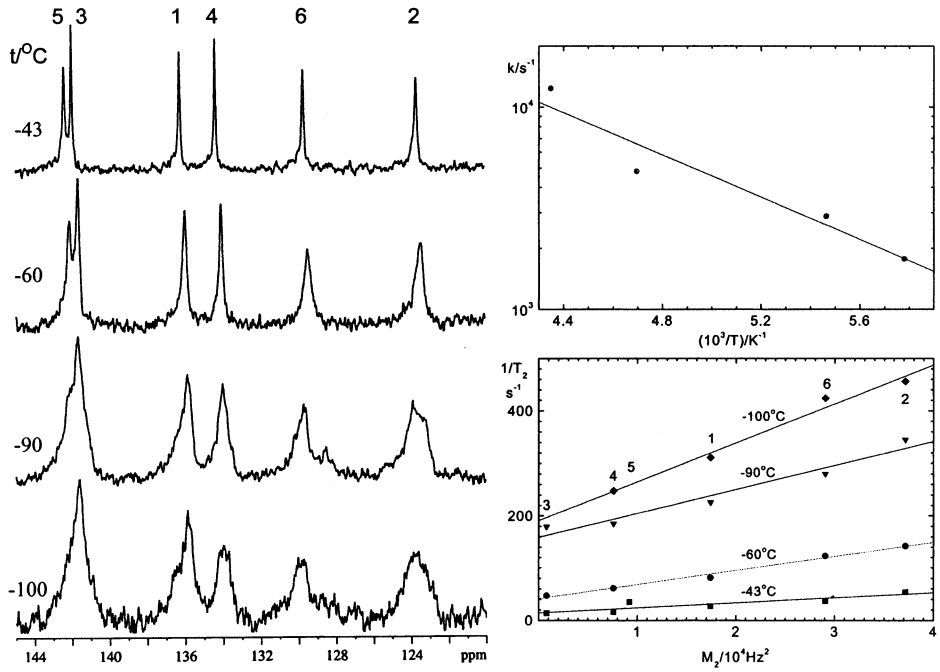


***Figure 14.*** Left: High-resolution carbon-13 NMR spectra of a solution of the saddle isomer of CTV-8 in $CD_2Cl_2$ at the indicated temperatures. Only the aromatic region is shown. The peak assignment is as in Figure 9. The assignment of peaks 3 and 5 is arbitrary and only made for identifying the plots on the bottom right side of the figure. Right bottom: Plots of the measured $1/T_2$ of the various aromatic carbons as measured from the spectra shown on the left side of the figure, as a function of their second moment (Table 3B). Due to signal overlap the results for carbons 3 and 5 are incomplete. Right top: Arrhenius plot of the pseudorotation rate constants derived from the results shown below.

on the NMR spectrum of the rigid crown form are expected on cooling. Yet on cooling, a solution of crown CTV-8 in $CD_2Cl_2$ to below −70 °C the various aromatic and carboxylic signals in the carbon-13 spectrum were found to split into a number of closely spaced peaks. Line splitting is also observed at low temperatures for the proton spectrum of the crown and, as discussed in Section 3.1, also for the saddle isomer. We believe that this effect reflects the formation of solute−solvent complexes at low temperatures. It is, in fact, known that CTV derivatives precipitate from solvents as crystalline inclusion compounds.[13] On the other hand, when the carbon-13 spectrum of the saddle isomer (of CTV-8) is recorded at low temperatures in the same solvent, rather than line splitting (or perhaps concomitant with the splitting) line broadening is observed. This is shown for the aromatic peaks on the left-hand side of Figure 14. We believe that this broadening reflects the slowing down of the pseudorotation and that the broadening conceals the splitting expected due to solute−solvent complexation. Indeed close examination of the spectra show unresolved structure which may be due to this effect.

The pseudorotation process amounts to averaging the triplets associated with the same type of carbons in the three inequivalent sites of the saddle conformer. To estimate the rate of the pseudorotation process, we recall that in the limit of fast exchange each of these triplets coalesces to a single line with a width[36]

$$\frac{1}{T_2} = \left(\frac{1}{T_2}\right)^0 + \left(\frac{1}{T_2}\right)^{ex} = \left(\frac{1}{T_2}\right)^0 + \nabla\tau \qquad (6)$$

where $(1/T_2)^{ex}$ is the contribution of the exchange to the line width and $(1/T_2)^0$ reflects all other, exchange-independent, contributions. The symbol $\nabla$, on the right-hand side of eq 6 stands for the "second moment" of the triplet of lines

$$\nabla^i = \frac{1}{3}(2\pi\nu_L)^2 \sum_l (\delta^{il} - \langle\delta^i_{iso}\rangle)^2 \qquad (7)$$

where the index $i$ labels the group of triplets, the index $l$ runs over the three carbons within the group, $\delta^{il}$ is their chemical shift and $\langle\delta_{iso}{}^i\rangle$ is their average shift. The correlation time, $\tau$, is related to the rate constant, $k_p$, for a single pseudorotation step by

$$\frac{1}{\tau} = 3k_p \qquad (8)$$

Assuming that the $\delta^{il}$ in the methylene chloride solution are the same as measured in the mesophase the second moments of the various types of carbons can be calculated. The results are included in Table 3B (and 3C). To proceed, we approximated the lines in the high-resolution spectra to Lorentzians and determine for each an effective $1/T_2$. These are plotted in the lower right side of Figure 14 as a function of the calculated second moment for the four measured temperatures (left-hand side of figure). It may be seen that the plots are fairly linear, suggesting that the $\nabla$-dependent parts indeed reflect the effect of pseudorotation. Also, the slope decreases with increasing temperature as would be expected for a thermally activated process. From the slope of these plots, using eqs 6 and 8, the rate constants for the reaction at the various temperatures were determined. The results are plotted in the upper right side of Figure 14 as a function of the inverse absolute temperature, yielding the following estimated kinetic parameters for the pseudorotation process

(36) Piette, L. H.; Anderson, W. A. *J. Chem. Phys.* **1959**, *30*, 899−908.

$k_p(-100\ °C) \approx 1.7 \times 10^3 s^{-1}$; $A \approx 1.8 \times 10^6\ s^{-1}$;

$E_a \approx 9.6$ kJ/mol; $\Delta S \approx -130\ JK^{-1}\ mol^{-1}$

Considering the uncertainty about the assumptions made and the lack of information about the spectral parameters of the frozen out saddle conformer at lower temperatures, these results should be considered as very tentative. However, the clear linear dependence of the line width on $\nabla$ provides support for the proposed model.

In the results described above, we note that the intercepts of the $1/T_2$ ves. $\nabla$ plots increase with lowering the temperature. These intercepts reflect the exchange-independent broadening mechanisms, in particular, the splitting referred to in the beginning of this section. These splittings apparently increase with decreasing temperature and are similar for the various types of carbons. They cannot, however, be observed for the saddle isomer because of the exchange broadening.

## 6. Summary and Conclusions

The CTV-*n* homologues exhibit a special form of mesomorphism due to the fact that they can exist in two isomeric forms, crown, and saddle. When substituted with sufficiently long side chains, both isomers are mesogenic exhibiting hexagonal columnar mesophases with similar lattice parameters. However, the saddle mesophase is thermodynamically less stable than that of the crown, as reflected in its lower clearing temperature and the fact that it slowly sublimes into the crown mesophase. NMR measurements indicate that the molecules in the crown mesophase reorient about the columns' axes, whereas in the saddle mesophase they are static. The higher mobility of the crown form within the mesophase can be understood on the basis of the packing modes of the molecules within the columns. The crown molecules can readily slip at their position, whereas the saddle molecules are stuck in the columns such as a pile of chairs (see schematic drawings of the crown (left) and saddle (right) columns in Figure 6). The stiffness exhibited by the saddle mesophase is quite unusual in the world of intermediate (in size) discotic liquid crystals.

The results of the present paper demonstrate the power of carbon-13 MAS NMR to study dynamic processes in the discotic liquid crystals. Dynamic measurements in such mesophase have extensively been performed in the ultraslow and dynamic linebroadening regime using deuterium NMR methods. The use of carbon-13 MAS has several advantages. In particular, selective labeling is not required because experiments can be carried out at natural abundance, and a single experiment provides information on different sites in the molecule. Also, the dynamic range of carbon-13 MAS is pushed down to slower rates since the natural line width of the MAS peaks is generally smaller than that of deuterium, whereas the upper limit of both methods is comparable.

**Acknowledgment.** This work was supported by the German-Israeli Foundation, G.I.F., Project No. I-558-218.05/97. We thank Professor H. -H. Limbach and Dr. Peter Tolstoy for performing preliminary low temperature NMR meaurements of saddle CTV-2 in Freon solutions.

JA020889E